



Age dependence of arterial pulse wave parameters extracted from dynamic blood pressure and blood volume pulse waves

Citation

Peltokangas, M., Vehkaoja, A., Verho, J., Mattila, V. M., Ronsi, P., Lekkala, J., & Oksala, N. (2015). Age dependence of arterial pulse wave parameters extracted from dynamic blood pressure and blood volume pulse waves. *IEEE Journal of Biomedical and Health Informatics*, 21(1), 142-149.
<https://doi.org/10.1109/JBHI.2015.2503889>

Year

2015

Version

Peer reviewed version (post-print)

Link to publication

[TUTCRIS Portal \(http://www.tut.fi/tutcris\)](http://www.tut.fi/tutcris)

Published in

IEEE Journal of Biomedical and Health Informatics

DOI

[10.1109/JBHI.2015.2503889](https://doi.org/10.1109/JBHI.2015.2503889)

Copyright

© 2015 IEEE. Personal use of this material is permitted. Permission from IEEE must be obtained for all other uses, in any current or future media, including reprinting/republishing this material for advertising or promotional purposes, creating new collective works, for resale or redistribution to servers or lists, or reuse of any copyrighted component of this work in other works.

Take down policy

If you believe that this document breaches copyright, please contact cris.tau@tuni.fi, and we will remove access to the work immediately and investigate your claim.

Age dependence of arterial pulse wave parameters extracted from dynamic blood pressure and blood volume pulse waves

Mikko Peltokangas, Antti Vehkaoja, Jarmo Verho, Ville M. Mattila, Pekka Ronsi, Jukka Leikkala, and Niku Oksala

Abstract—Atherosclerosis is a significant cause of mortality in the aged population, and it affects arterial wall properties causing differences in measured arterial pulse wave (PW). In this study, both dynamic arterial blood pressure PWs and blood volume PWs are analyzed. The PWs are recorded non-invasively from multiple measurement points from the upper and lower limbs from 52 healthy (22–90-year-old) volunteers without known cardiovascular diseases. For each signal, various parameters earlier proposed in literature are computed, and 25 different novel parameters are formed by combining these parameters. The results are evaluated in terms of age and heart rate (HR) dependence of the parameters. In general, the results show that 14 out of 25 tested combined parameters have stronger age dependence than any of the individual parameters. The highest obtained linear correlation coefficients between the age and combined parameter and individual parameter equal to 0.85 ($p < 10^{-4}$) and 0.79 ($p < 10^{-4}$), respectively. Most of the combined parameters have also improved discrimination capability when classifying the test subjects into different age groups. This is a promising result for further studies, but indicate that the age dependence of the parameters must be taken into account in further studies with atherosclerotic patients.

Index Terms—Atherosclerosis, Body sensor networks, Electromechanical sensors, Photoplethysmography, Pulse wave measurements

I. INTRODUCTION

CARDIOVASCULAR diseases due to atherosclerosis are an increasing cause of disabilities and mortality and they are challenging to detect due to their subclinical course [1]–[3]. To detect subclinical atherosclerosis and to reduce morbidity and mortality, cost-effective methods for monitoring the vasculature are needed. Traditional methods include the

measurement of electrocardiogram (ECG), instantaneous systolic and diastolic blood pressures and different indices such as ankle-brachial pressure index (ABI) [2].

Arterial pulse wave (PW) carries plenty of information on the vascular health, but this information is not yet commonly utilized in the clinical medicine. The arterial PW observed at a peripheral measurement point such as a finger is a superposition of a percussion wave induced by the heartbeat and its reflections from the impedance discontinuities of the main artery, aorta [4]. The propagation velocity of these waves, both percussion wave and its reflections, depends on arterial elasticity which is an important indicator of the vascular health, especially the degree of atherosclerosis, which characteristically results in arterial stiffening. Depending on the propagation velocity and thus the arrival times of the reflections, the observed PW looks different: the stiffer the arteries are, the earlier the reflections arrive to the peripheral measurement point. Various methods have been developed for detecting the specific features of the PWs and thus for evaluating the arterial condition [4]–[12] but these methods are still mainly used for research purposes. Although atherosclerosis is the most probable cause of arterial stiffening during aging, it is possible that also other factors contribute to this phenomenon. Atherosclerosis may present as stiffening, stenosis or occlusion of the vessels and only hemodynamically severe and significant stenoses result in symptoms and alterations of ABI.

There is a growing need to develop clinically applicable, noninvasive, rapid and cheap methodology to detect arterial diseases. In this paper, we present methods for analyzing the PWs recorded from multiple measurement points with two different sensor modalities: volume pulse waves recorded using optical photoplethysmographic (PPG) sensors (index finger and second toe) and dynamic pressure pulse waves recorded with the sensors made of electromechanical film (EMFi) (wrist, cubital fossa and ankle). In addition to computing individual PW parameters, we pilot combining the information obtained from multiple measurement points for obtaining better discrimination capability between the subjects of different age groups. The age dependence of the PW parameters is an important subject for study since arteries tend to degenerate due to aging and the prevalence of the atherosclerotic changes is also related to aging. Age is also a potential confounder since there are several other risk factors for atherosclerotic changes. For these reasons, we sought to study the age-

Manuscript received on June 9, 2015; revised on October 20, 2015; accepted on November 18, 2015. Date of publication XXmonth ZZ, YYYY; date of current version November 24, 2015. The work was funded by the Finnish Funding Agency for Technology and Innovation (TEKES) as a part of project VitalSens (decision ID 40103/14), Doctoral Programme of the President of the Tampere University of Technology, and grants from Finnish Cultural Foundation/Pirkanmaa Regional Fund/Elli and Elvi Oksanen's Fund and Tekniikan edistämissäätiö.

M. Peltokangas, A. Vehkaoja, J. Verho, and J. Leikkala are with Tampere University of Technology, Department of Automation Science and Engineering, BioMediTech, Tampere, Finland (e-mail: mikko.peltokangas@tut.fi; antti.vehkaoja@tut.fi; jarmo.verho@tut.fi; jukka.leikkala@tut.fi).

V.M. Mattila and N. Oksala are with Tampere University Hospital, Tampere, Finland, and University of Tampere (School of Medicine, Surgery), Tampere, Finland (e-mail: niku.oksala@pshp.fi; ville.mattila@uta.fi).

P. Ronsi is with Oulu University Hospital, Oulu, Finland (e-mail: pekka.ronsi@ppshp.fi).

dependence of different PW parameters describing the arterial aging for testing our novel technology with healthy volunteer test subjects. Besides the age-dependence analysis of the tested PW parameters, their dependence on subject's heart rate (HR) is analyzed.

II. RELATED STUDIES

In clinical medicine, a gold standard for the detection of atherosclerosis is the ABI measurement [2]. However, abnormal $ABI < 0.9$ does not necessarily reveal the atherosclerosis before the disease has developed from arterial stiffening into stenosis or occlusions. Still, there are practically no simple and cost-effective options for vascular evaluation, although several authors have proposed various analysis and measurement methods for the arterial PW analysis. The data for the PW analysis is most commonly collected as a pressure pulse from the radial or carotid artery by using a tonometric sensor [7], [8], or as a volume pulse by using index finger PPG [5], [6]. In the tonometric technique, a pressure transducer is placed on top of a superficial artery so that the artery is applanated. In the PPG technique, the varying peripheral blood volume modifies the absorption or reflection coefficient of the tissue in optical pathway of the light, and this is observed by measuring the transmitted or reflected light intensity. These different methods do not provide exactly equivalent signals because not only the measurement points are usually different, but also because the peripheral blood pressure and volume depend non-linearly on each other [5].

In the analysis point of view, peripheral augmentation indices (pAIx) as the ratio of second and first systolic peak amplitudes have often been used in the pressure PW analysis [7], [8]. For the PPG signal analysis, Takazawa *et al.* have proposed a parameter called aging index (AGI), which is based on the first five local extremities of the second derivative of index finger PPG [6]. Other PPG-based indices found from literature are reflection index (RI) as the ratio of diastolic and systolic peak amplitudes and stiffness index (SI) as the ratio of patient's height and the time delay t_{pp} between the systolic and diastolic peaks [5], [9].

In recent years, several pulse wave decompositions have also been proposed due to increased computational capabilities [5], [10]–[12]. In PW decomposition, the measured PW is decomposed into 2–5 highly non-linear components that model the percussion wave and its reflections. However, there are several major drawbacks with PW decompositions based on iterative non-linear optimization procedures, such as their computational complexity and ambiguity of the results.

III. MATERIALS AND METHODS

A. Measurement hardware and sensor placement

All the signals were measured by using a synchronous wireless body sensor network [13]. The PPG signals were sampled at 500 Hz, whereas ECG and dynamic pressure signals recorded with EMFi sensors were sampled by using a sampling frequency of 250 Hz. However, the signals sampled at 250 Hz were interpolated to 500 Hz before further data processing for obtaining better temporal resolution and having

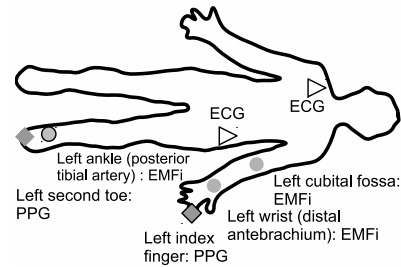


Figure 1. Pulse wave sensor placement.

the same sampling frequency for all the signals in later signal processing steps.

The sensor placement is illustrated in Fig. 1. The PPG-probes illuminating the tissue with 905 nm infrared light were located on left index finger and left second toe for collecting volume PW signals. The dynamic pressure PWs were recorded with EMFi sensors placed on left ankle (posterior tibial artery), left wrist (left distal antebrachium / radial artery) and left cubital fossa (brachial artery). In addition, bipolar ECG was recorded from the subjects by conventional disposable ECG electrodes located under the right clavicle and left lower abdomen.

B. Study subjects

The PW signals were recorded from 52 volunteer test subjects (30 men and 22 women) who did not have symptoms of atherosclerosis or diagnosed arterial diseases. Ankle-brachial pressure index (ABI) was recorded from all the test subjects and the test subject candidates having abnormal ABI ($ABI < 0.9$ or $ABI > 1.3$) were excluded from this study. The measurements were conducted in Tampere University Hospital (Tampere, Finland), Oulu University Hospital (Oulu, Finland) and in Tampere University of Technology (Tampere, Finland). The patient measurements were accepted by the local ethical committees of the hospital districts (decision IDs R14096 and 69/2014 245§) and the Finnish National Supervisory Author of Health and Welfare (Valvira, ID 272). All volunteer test subjects were informed on the purpose of the study and the informed consents were obtained. The subjects also had a chance to ask further information and interrupt their participation at any point without reasoning.

In the analysis, the 22–90-year-old test subjects were divided into three age groups: group A as ≤ 40 years, group B as 41–69 years and group C as ≥ 70 years. Groups B and C were formed by dividing the elder test subjects into two groups, whereas group A is slightly more distinct subpopulation with respect the age. The number of test subjects being in each age group and having different cardiovascular risk factors are shown in Table I.

C. Signal preprocessing

All the signal processing was done offline in MATLAB (version R2014b) environment. In preprocessing stage, the signals were synchronized based on the time stamps of each data point. After the synchronization, the signals were filtered with a Savitzky-Golay (SG) smoothing filter having a window

Table I
NUMBER OF PATIENTS HAVING DIFFERENT CARDIOVASCULAR RISK
FACTORS IN EACH AGE GROUP.

Age group	Age (mean \pm std)	Instantaneous HR (mean \pm std) (bpm)	Number of subjects	Diabetes	Dyslipidemia	Smoking	Raynaud's phenomenon	Rheumatoid arthritis	Hypertension
A: ≤ 40	29.6 \pm 4.6	54.7 \pm 10.2	12	1	0	0	0	1	0
B: 41–69	61.5 \pm 6.9	54.8 \pm 8.4	19	1	2	3	1	1	3
C: ≥ 70	76.5 \pm 5.2	52.7 \pm 10.6	21	1	3	4	3	4	4
Σ : 22–90	60.2 \pm 19.1	53.9 \pm 9.8	52	3	5	7	4	6	7

length of 91 samples and a polynomial order of 2. In addition, the signals were lowpass-filtered with a finite impulse response (FIR) filter having a cut-off-frequency of 10 Hz, transition band of 10 Hz–12 Hz, pass band ripple of 0.05 dB and stop band attenuation of 100 dB, as proposed in [14]. The relatively heavy filtering is required since the features detected in the parameter extraction are based on high-order derivatives of the PW signals. However, this does not significantly affect to the shape of PW contour, as seen in the examples shown in Fig. 2.

The individual PWs were detected by using the R-peaks found from the recorded ECG signal as a marker of heartbeats: the last local minimum after the R-peak and before the steepest rise of the PW was considered as a boundary between two consecutive PWs.

D. Pulse wave parameter extraction

For each PW from each measurement channel, four traditional pulse wave parameters were defined based on the PW contour and its derivatives: pAIx, RI, t_{pp} and AGI. Before the parameter extraction, a linear trend fixed to the end points was subtracted from each individual PW.

For the parameter determination, let the i^{th} individual PW be $f_i = [y_{i,1}, y_{i,2}, \dots, y_{i,N}]$ and $f'_i, f''_i, f'''_i, f_i^{(4)}$, and $f_i^{(5)}$ its 1st, 2nd, 3rd, 4th, and 5th derivatives approximated by discrete differences, respectively. As the first step, the maximum of f_i is detected. Next, a point of incisura dividing the PW into systolic and diastolic parts is searched. This is detected as the last zero-crossing from negative to positive of f'_i in the search window limited by a point 80 ms after the maximum of f_i and a point which corresponds to 65% from the total length of the PW. In case of the absence of such zero-crossing of f'_i , the location of incisura is detected at the location of the highest peak of f''_i found from the same interval. Examples illustrating the detection of incisura are shown in Fig. 2 for both cases.

1) *RI and t_{pp}* : RI is defined as the ratio of diastolic and systolic peak amplitudes B and A as

$$RI = \frac{B}{A}. \quad (1)$$

Peak-to-peak time t_{pp} is defined as the time delay between the systolic and diastolic peaks A and B , respectively. The graphical explanations for A and B are shown in Fig 2.

However, especially with clinically interesting cases i.e. people with vascular diseases, the location and the amplitude

of the diastolic peak is often everything but clear and obvious. If there is a clear diastolic local maximum, i.e. there is a zero-crossing of f'_i from positive to negative in the diastolic part of the PW, this point is selected as the location of the diastolic peak. If such diastolic zero-crossing of f'_i is missing, the location for the diastolic peak is defined as the first zero-crossing of f''_i from positive to negative in the diastolic part of the PW. This point corresponds to a point in which the f'_i is closest the zero. [14]

2) *pAIx*: The basic idea behind pAIx proposed e.g. in [8] is to calculate the parameter as the ratio of the amplitudes of late and early systolic peaks as

$$pAIx = \frac{P_2}{P_1}. \quad (2)$$

However, the two overlapping peaks are often indistinguishable from each other. For this reason, fourth order derivative analysis is needed for revealing the location of hidden systolic peak as proposed in [15]: If the sign of the $f_i^{(5)}$ (i.e. the slope of $f_i^{(4)}$) at the point corresponding to the systolic maximum of PW is

- 1) positive, this point is considered as a point for the late systolic peak P_2 and the last zero-crossing of $f_i^{(4)}$ from positive to negative before P_2 as early systolic peak P_1 .
- 2) negative, this point is considered as a point for the early systolic peak P_1 and the first zero-crossing of $f_i^{(4)}$ from negative to positive after P_1 as a late systolic peak P_2 .

The detection of early and late systolic peaks is illustrated in Fig. 2 for different kind of cases: the left side panels are for case 2 and the right side panels for case 1.

3) *AGI*: AGI is calculated based on its definition [6] by using the amplitudes of the first five extremities of f''_i as

$$AGI = \frac{b - c - d - e}{a} \quad (3)$$

in which a is the maximum of f''_i and $b, c, d,$ and e are the following local extremities (both peaks and troughs) of f''_i .

E. Outlier replacement in the time series of the parameters

Because of derivative-based feature extraction algorithms and artefact-containing signals, the time-series of the computed parameters contain occasionally outliers. In order to remove the outliers, parameters related to the PWs observed at different measurement points and caused by each j^{th} heart beat were organized as feature vectors $\mathbf{x}_j = [x_1, x_2, \dots, x_n]^T \in \mathbb{R}^n$ where each x_i represents the value of one arterial index from one measurement point. Because the total number of PW measurement points is 5 and 4 parameters are determined for each measurement point, each \mathbf{x}_j has 20 elements. The feature vectors of each test subject k were gathered into a matrix $\mathbf{X}_k = [\mathbf{x}_1, \mathbf{x}_2, \dots, \mathbf{x}_m]^T \in \mathbb{R}^{m \times n}$ where m refers to the number of heart beats. Due to motion artefacts, all measurement channels cannot provide useful signal all the time, so the missing values of each time series were replaced by its median. The outliers of the time-series (columns) in \mathbf{X}_k were replaced by using a winsorizing and principal component analysis based multivariate method proposed in [16] and by implementing Huber's M-estimator with parameter values of $k = 1.5$ and $\epsilon = 10^{-5}$.

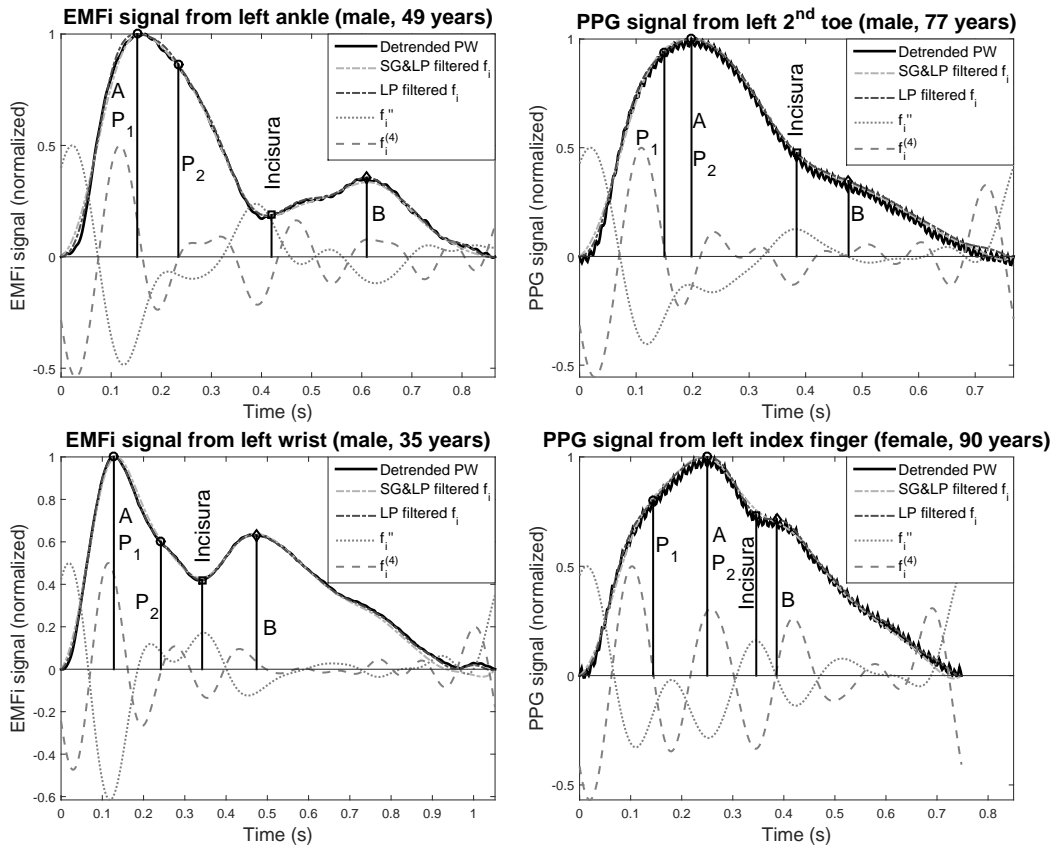


Figure 2. Detrended PW without any digital filtering, both Savitzky-Golay (SG) and low-pass (LP) filtered PW and only low-pass filtered PW for different kind of pulse waves. Also 2nd and 4th order derivatives based on SG&LP filtered PWs are shown. In each figure, the two leftmost characteristic points are for pAIx determination and the two rightmost characteristic points are for the determination of incisura and dirotic wave.

F. Combined parameters

The single parameters may have high beat-to-beat variation and different parameters may provide sometimes inconsistent information on the vascular health or be skewed systematically because the particular features of the PW may be ambiguous with some individuals. Earlier, only a sensor modality and measurement point specific analysis methods have been proposed [5]–[12] although additional measurement points may provide different perspective to the PW analysis. In addition, valuable information could be extracted from the data by computing multiple parameters from the PW and condensing them as a new more representative index.

The leading hypothesis behind the combined parameters is to reduce the uncertainty of the results by increasing the amount of correlating measurements of the same phenomenon with independent and random variations and therefore improving the signal-to-noise ratio of the result. We tested all the possible combinations that can be formed by averaging the individual parameters in the same scale as

$$I_j = \frac{1}{N} \sum_{z_i \in \Omega} z_i \quad (4)$$

where z_i refers to the selected outlier-corrected individual parameters, Ω is the set of the selected parameters and N is the the number of selected parameters. Therefore, 25 different groups of different combinations are formed (and the

results I_j are subscripted) as follows: groups 1–4 include all combinations containing pAIx values from 2–5 measurement points; groups 5–8 include all combinations containing RI values from 2–5 measurement points; groups 9–12 include all combinations containing t_{pp} values from 2–5 measurement points; groups 13–16 include all combinations containing AGI values from 2–5 measurement points; and groups 17–25 include all combinations containing 2–10 pAIx or RI values. The explanations for the selected combined parameters I_j are shown in Tables II–III, and the number of possible combinations in each groups varies between 1 and 252.

If the individual parameters from different scales were combined (such as t_{pp} and interval-scaled AGI), the input data should be normalized before the analysis. However this is not a straightforward process because of non-fixed endpoints of the parameter ranges. For this reason, we combined only the parameters already being in the same scale, but the techniques that can be utilized in constructing more advanced models are included in our future interests.

G. Age dependence

The age dependence of the individual and combined parameters were studied both based on the mean values of each parameter as well as based on the parameter values obtained from individual PWs.

As the number of test subjects in each age group is only 12–21, two-sided Mann-Whitney U-tests are implemented to

Table II
INDIVIDUAL PARAMETERS (Ω) USED IN THE DETERMINATION OF COMBINED PARAMETERS I_j . THE EXPLANATIONS FOR THE ITEMS IN Ω ARE SHOWN IN THE FIRST COLUMN OF TABLE III.

j	Set of individual parameters, Ω_j	Set of individual parameters, Ω
1	$\{W_p, F_p\}$	14 $\{W_A, F_A, T_A\}$
2	$\{W_p, F_p, T_p\}$	15 $\{W_A, C_A, F_A, T_A\}$
3	$\{W_p, A_p, F_p, T_p\}$	16 $\{W_A, C_A, A_A, F_A, T_A\}$
4	$\{W_p, C_p, A_p, F_p, T_p\}$	17 $\{W_p, F_p\}$
5	$\{A_R, T_R\}$	18 $\{W_p, F_p, T_R\}$
6	$\{A_R, F_R, T_R\}$	19 $\{W_p, A_R, F_p, T_R\}$
7	$\{W_R, A_R, F_R, T_R\}$	20 $\{W_p, A_p, F_p, T_p, T_R\}$
8	$\{W_R, C_R, A_R, F_R, T_R\}$	21 $\{W_p, C_p, A_p, F_p, T_p, T_R\}$
9	$\{F_t, T_t\}$	22 $\{W_p, C_p, A_p, A_R, F_p, T_p, T_R\}$
10	$\{A_t, F_t, T_t\}$	23 $\{W_p, C_p, A_p, A_R, F_p, F_R, T_p, T_R\}$
11	$\{C_t, A_t, F_t, T_t\}$	24 $\{W_p, W_R, C_p, A_p, A_R, F_p, F_R, T_p, T_R\}$
12	$\{W_t, C_t, A_t, F_t, T_t\}$	25 $\{W_p, W_R, C_p, C_R, A_p, A_R, F_p, F_R, T_p, T_R\}$
13	$\{F_A, T_A\}$	$\{T_R\}$

check whether there are statistically significant differences in the parameter values found for different age groups. In the statistical testing, p -values less than 0.05 are considered as statistically significant.

H. HR dependence

The varying HR of a subject or between subjects is a potential confounder of the analysis because the duration of the PW affects also the peak amplitudes of the PW. Therefore we computed the correlation coefficients between the instantaneous HR and the parameter values. This analysis was performed for each individual test subject for each tested parameter in order to check the intra-subject parameter value dependence on HR. The average correlation coefficients and their standard deviations are reported as results from this test. We also calculated the correlation coefficients between each test subject's average HR and average parameter values in order to study the inter-subject variability of the parameter values due to HR.

IV. RESULTS

A. Correlation between age and parameter value

Pearson's product moment correlation coefficient between the age and PW parameter values are shown in Table III for both individual parameter values as well as combined parameter values. The results of correlation analysis are shown for both averaged parameter values as well as for parameter values based on individual PWs. The age-dependence of the combined parameters is graphically illustrated with regression lines in Fig. 3 for the averaged data. The maximum absolute values of the Pearson's correlation coefficient between the age and individual parameter values are below 0.80, being 0.71–0.79 ($p < 10^{-4}$) and many individual parameters have practically no correlation with age. However, higher correlation coefficients are found for the selected combined parameters $I_1 - I_{25}$. The maximum obtained correlation coefficient of the combined parameters equals 0.85 ($p < 10^{-4}$).

Similarly as with Pearson's correlation coefficient, the results for the analysis of Spearman's rank correlation coefficient

Table III
TWO DIFFERENT CORRELATION COEFFICIENTS FOR AGE DEPENDENCE, PEARSON'S r FOR AGE-PARAMETER AND SPEARMAN r FOR AGE GROUP-PARAMETER DEPENDENCE. ALSO THE CORRELATION COEFFICIENTS BETWEEN HR AND PARAMETER VALUES ARE SHOWN FOR INTRA- AND INTER-SUBJECT HR DEPENDENCE.

S or G	Parameter	Age dependence				HR dependence		
		Pearson's r		Spearman's r		Intra-subject r	Inter-subject r	
		Aver. r	Indiv. r	Aver. $ r $	Indiv. $ r $	mean \pm std		
W_p	pAlx	0.76*	0.74*	0.63*	0.63*	-0.20 \pm 0.20	-0.11	
W_R	RI	0.04	0.08*	0.05	0.08*	-0.23 \pm 0.26	0.28 \oplus	
W_t	t_{pp}	-0.37 \ddagger	-0.40*	0.47 \ddagger	0.47*	-0.01 \pm 0.18	0.33 \oplus	
W_A	AGI	0.64*	0.62*	0.57*	0.56*	-0.15 \pm 0.19	-0.22	
C_p	pAlx	0.63*	0.63*	0.56*	0.56*	-0.16 \pm 0.23	-0.11	
C_R	RI	-0.13	-0.06*	0.04	0.10*	-0.20 \pm 0.25	0.22	
C_t	t_{pp}	-0.48 \ddagger	-0.51*	0.50 \ddagger	0.51*	-0.02 \pm 0.19	0.39 \ddagger	
C_A	AGI	0.49 \ddagger	0.47*	0.53*	0.50*	-0.10 \pm 0.20	-0.10	
A_p	pAlx	0.52*	0.53*	0.35 \oplus	0.37*	-0.05 \pm 0.13	-0.02	
A_R	RI	0.47 \ddagger	0.50*	0.50 \ddagger	0.51*	-0.17 \pm 0.24	0.07	
A_t	t_{pp}	-0.59*	-0.59*	0.48 \ddagger	0.51*	-0.02 \pm 0.18	0.51 \ddagger	
A_A	AGI	0.36 \ddagger	0.35*	0.37 \ddagger	0.40*	-0.02 \pm 0.13	-0.11	
F_p	pAlx	0.79*	0.78*	0.68*	0.67*	-0.20 \pm 0.21	-0.10	
F_R	RI	0.10	0.14*	0.24	0.24*	-0.22 \pm 0.26	0.50 \ddagger	
F_t	t_{pp}	-0.78*	-0.77*	0.68*	0.66*	0.05 \pm 0.18	0.14	
F_A	AGI	0.71*	0.71*	0.65*	0.64*	-0.15 \pm 0.16	-0.17	
T_p	pAlx	0.59*	0.58*	0.70*	0.65*	-0.10 \pm 0.18	-0.03	
T_R	RI	0.46 \ddagger	0.46*	0.54*	0.50*	-0.24 \pm 0.29	0.29 \oplus	
T_t	t_{pp}	-0.64*	-0.65*	0.64*	0.63*	-0.04 \pm 0.22	0.23	
T_A	AGI	0.41 \ddagger	0.39*	0.43 \ddagger	0.37*	-0.07 \pm 0.19	-0.11	
	pAlx	I_1	0.81*	0.80*	0.66*	0.67*	-0.23 \pm 0.20	-0.10
		I_2	0.83*	0.82*	0.71*	0.71*	-0.23 \pm 0.20	-0.08
		I_3	0.84*	0.83*	0.70*	0.70*	-0.21 \pm 0.20	-0.06
		I_4	0.82*	0.82*	0.69*	0.69*	-0.23 \pm 0.21	-0.06
	RI	I_5	0.59*	0.61*	0.59*	0.59*	-0.24 \pm 0.26	0.24
		I_6	0.50 \ddagger	0.53*	0.53*	0.55*	-0.27 \pm 0.28	0.39 \ddagger
		I_7	0.43 \ddagger	0.47*	0.48 \ddagger	0.50*	-0.29 \pm 0.28	0.42 \ddagger
		I_8	0.33 \oplus	0.38*	0.43 \ddagger	0.44*	-0.30 \pm 0.28	0.44 \ddagger
	t_{pp}	I_9	-0.79*	-0.78*	0.70*	0.70*	-0.00 \pm 0.23	0.21
		I_{10}	-0.80*	-0.80*	0.67*	0.68*	-0.01 \pm 0.21	0.37 \ddagger
		I_{11}	-0.75*	-0.76*	0.66*	0.67*	-0.01 \pm 0.21	0.40 \ddagger
		I_{12}	-0.70*	-0.72*	0.65*	0.65*	-0.01 \pm 0.22	0.39 \ddagger
	AGI	I_{13}	0.76*	0.74*	0.69*	0.68*	-0.13 \pm 0.19	-0.19
		I_{14}	0.78*	0.76*	0.69*	0.68*	-0.17 \pm 0.20	-0.21
		I_{15}	0.78*	0.76*	0.71*	0.70*	-0.18 \pm 0.22	-0.20
		I_{16}	0.75*	0.74*	0.70*	0.69*	-0.15 \pm 0.20	-0.18
	pAlx & RI	I_{17}	0.81*	0.80*	0.66*	0.67*	-0.23 \pm 0.20	-0.10
		I_{18}	0.83*	0.82*	0.75*	0.73*	-0.27 \pm 0.25	0.02
		I_{19}	0.84*	0.83*	0.73*	0.72*	-0.28 \pm 0.24	0.04
		I_{20}	0.85*	0.84*	0.75*	0.74*	-0.24 \pm 0.24	0.01
		I_{21}	0.85*	0.84*	0.74*	0.73*	-0.25 \pm 0.24	-0.00
		I_{22}	0.85*	0.84*	0.73*	0.72*	-0.26 \pm 0.24	0.01
		I_{23}	0.82*	0.82*	0.70*	0.72*	-0.28 \pm 0.25	0.08
		I_{24}	0.80*	0.79*	0.69*	0.69*	-0.29 \pm 0.26	0.11
		I_{25}	0.75*	0.75*	0.66*	0.66*	-0.29 \pm 0.26	0.14

*: $p < 10^{-4}$, \ddagger : $p < 10^{-3}$, \ddagger : $p < 0.01$, \oplus : $p < 0.05$. S or G: Symbol of the individual parameter or the parameter group in which the combined parameter is based on. Cubit. F. = cubital fossa

between the parameter values and the age groups presented in Table I are shown in Table III. The highest Spearman's correlation coefficient obtained for the individual parameters equals to 0.70 ($p < 10^{-4}$). As seen in Table III, higher correlations are again obtained with the combined parameters, being 0.70–0.75 ($p < 10^{-4}$).

B. Differences between different age groups

The results of the statistical tests between different age groups are shown in Table IV for the individual and combined parameters. The distributions of the averaged data are also illustrated with boxplots in Fig. 4 for both types of parameters.

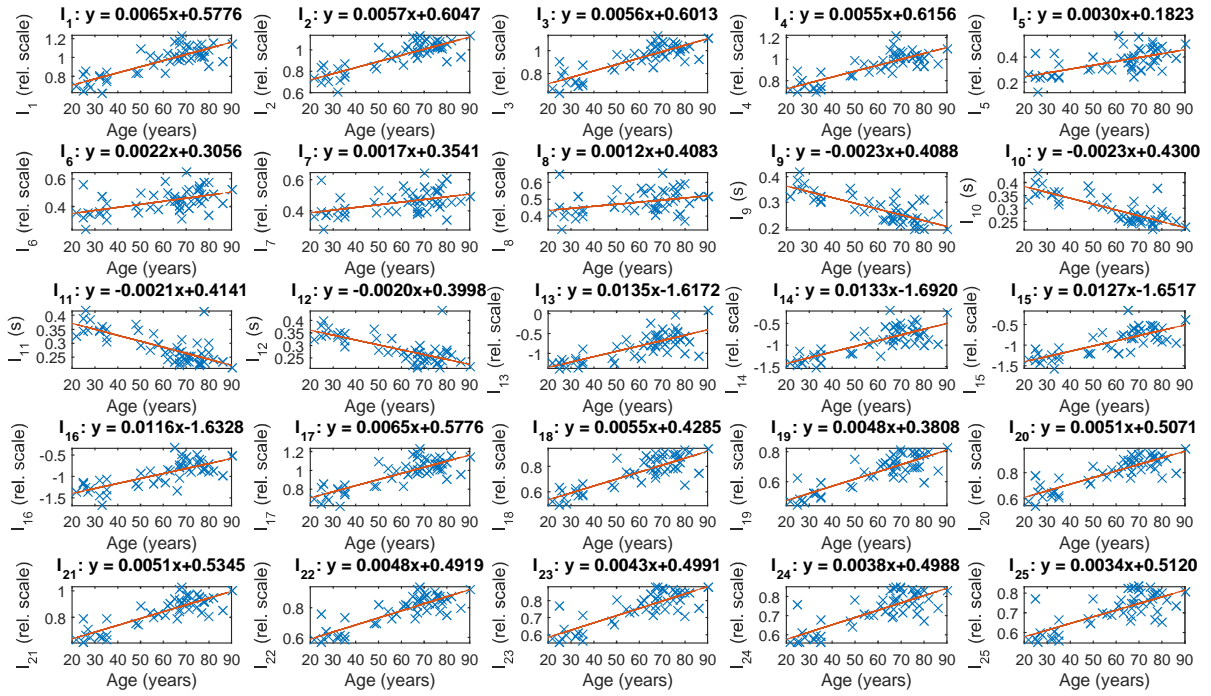
Figure 3. Scatter plots, regression lines and their coefficients for the combined parameters I_1 – I_{25} .

Table IV

THE p -VALUES FOR THE REJECTION OF THE NULL HYPOTHESES OF THE TWO-SIDED MANN-WHITNEY U-TESTS FOR THE INDIVIDUAL AND COMBINED PARAMETERS BETWEEN DIFFERENT AGE GROUPS.

Param.	Combined parameters		i	Individual parameters	
	A vs. B	B vs. C		A vs. B	B vs. C
I_1	$< 10^{-4}$	NS	W_p	$< 10^{-4}$	NS
I_2	$< 10^{-4}$	NS	W_R	NS	NS
I_3	$< 10^{-4}$	NS	W_t	$< 10^{-3}$	NS
I_4	$< 10^{-4}$	NS	W_A	$< 10^{-4}$	NS
I_5	$< 10^{-2}$	< 0.05	C_p	$< 10^{-4}$	NS
I_6	< 0.05	< 0.05	C_R	NS	NS
I_7	< 0.05	NS	C_t	$< 10^{-3}$	NS
I_8	< 0.05	NS	C_A	< 0.05	NS
I_9	$< 10^{-3}$	$< 10^{-2}$	A_p	< 0.05	NS
I_{10}	$< 10^{-3}$	< 0.05	A_R	$< 10^{-2}$	NS
I_{11}	$< 10^{-3}$	< 0.05	A_t	$< 10^{-2}$	NS
I_{12}	$< 10^{-3}$	NS	A_A	NS	NS
I_{13}	$< 10^{-4}$	< 0.05	F_p	$< 10^{-4}$	< 0.05
I_{14}	$< 10^{-4}$	NS	F_R	NS	NS
I_{15}	$< 10^{-4}$	NS	F_t	$< 10^{-3}$	< 0.05
I_{16}	$< 10^{-3}$	< 0.05	F_A	$< 10^{-3}$	NS
I_{17}	$< 10^{-4}$	NS	T_p	$< 10^{-2}$	$< 10^{-2}$
I_{18}	$< 10^{-4}$	$< 10^{-2}$	T_R	< 0.05	$< 10^{-2}$
I_{19}	$< 10^{-4}$	< 0.05	T_t	$< 10^{-2}$	$< 10^{-2}$
I_{20}	$< 10^{-4}$	$< 10^{-2}$	T_A	NS	NS
I_{21}	$< 10^{-4}$	< 0.05	A, B, and C refer to the age groups presented in Table I. The column header i refers to the individual parameters presented in Table III. NS = not significant, i.e. $p \geq 0.05$.		
I_{22}	$< 10^{-4}$	< 0.05			
I_{23}	$< 10^{-4}$	< 0.05			
I_{24}	$< 10^{-4}$	NS			
I_{25}	$< 10^{-3}$	NS			

C. HR dependence

The averages of the correlations between test subject's instantaneous HR and parameter values are presented in Table III as intra-subject HR-dependence. The absolute value of each correlation coefficient is less than 0.3, but the standard deviations are quite high, being 0.29 in maximum. The maximum

correlations between the averaged HR and parameter values (inter-subject HR dependence) equal to 0.51 and 0.44 for the individual and combined parameters, respectively.

V. DISCUSSION

A. Age dependence

In this study, we showed that combining the data from multiple measurement points may provide additional information for arterial screening. Although there are parameter values with strong age dependence, it does not automatically guarantee that those particular parameters are versatile in discriminating the healthy arteries from e.g. the arteries having atherosclerotic changes. However, the arteries tend to degenerate with age and the probability of atherosclerosis is linked to age, so the parameters having strong age dependence are promising startpoints for a study where differences between healthy control subjects and e.g. atherosclerotic patients are studied. It is also possible that the obtained regression equations (Fig. 3) can be utilized in compensating the effects of age or checking whether a particular PW parameter value is normal with respect to patient's age.

According to the results, the highest age-parameter value correlations and the best discrimination capability between different age groups are seen with the combined parameters that are composed of the individual PW parameters based on the signals recorded from both upper and lower limbs, such as I_{18} – I_{23} .

Only few reference values are available for comparing the obtained Pearson's correlation coefficients since the parameters have previously been tested only for a single measurement point and method. Takazawa *et al.* [6] reported a correlation coefficient of 0.80 ($p < 10^{-3}$) for the index finger based AGI, whereas a correlation of 0.71 ($p < 10^{-4}$) was obtained in this

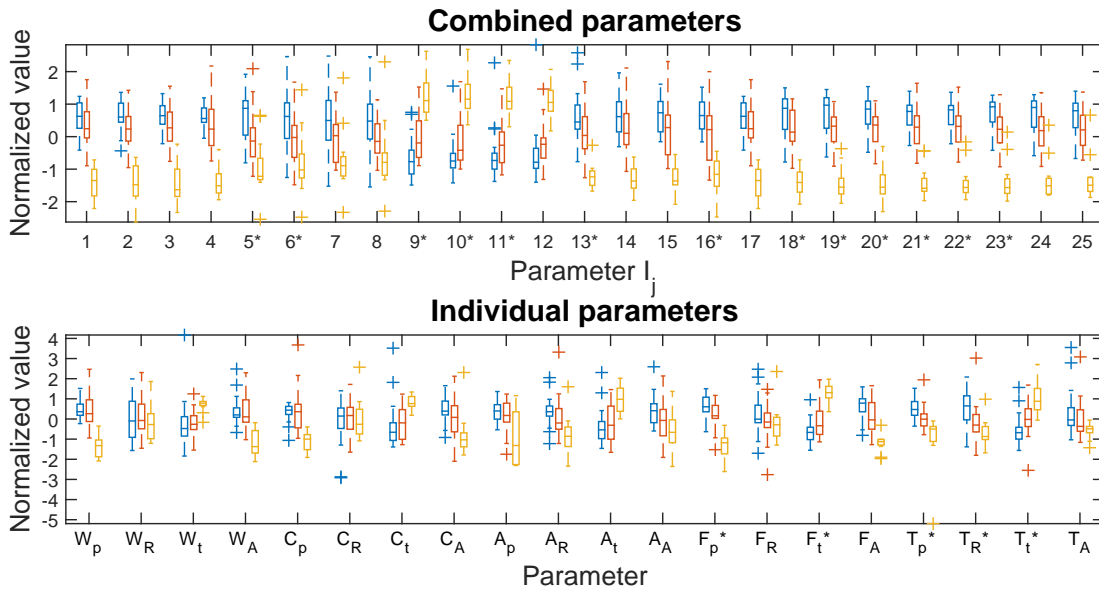


Figure 4. Distributions of different indices for each age group for both combined parameters (upper panel) and individual parameters (lower panel). Each group of three boxplots represents different arterial index and the joint distribution of each parameters are normalized. The order from left to right in each group is ≥ 70 -year-old (blue), 40–69-year-old (red) and < 40 -year-old (yellow) test subjects. For the parameters marked with *, $p < 0.05$ for all groups.

study. Kohara *et al.* [7] have reported correlation coefficients of 0.619 ($p < 10^{-3}$) and 0.644 ($p < 10^{-3}$) for men and women, respectively, between the wrist pAIx and the age. In this study, higher correlations, 0.76 ($p < 10^{-4}$) and 0.74 ($p < 10^{-4}$) were obtained for wrist pAIx values based on averaged data and individual PWs, respectively. The gender based analysis was not performed in this study since the sex ratio does not follow the uniform distribution especially in the youngest test subject group A.

Related to index finger PPG based t_{pp} , Pearson's correlations of -0.78 ($p < 10^{-4}$) (averaged data) and -0.77 ($p < 10^{-4}$) (individual PWs) were achieved in this study. These are somewhat higher than the correlations coefficients reported in [14], 0.63 ($p < 10^{-3}$) for a parameter called stiffness index which depends on t_{pp} inversely. In the same study, a correlation coefficient of 0.24 was reported between the age and index finger PPG based RI. Low age dependence of index finger RI is supported also by this study, since insignificant correlation of 0.10 was found. However, the RIs based on the lower limb signals have clearly higher linear age dependencies in this study ($r = 0.46$ – 0.50 for ankle and toe PW based signals) than those ones computed based on upper limb signals. The reflection causing the PW features detected as a reflected diastolic wave in the RI determination have at least different arterial pathways and possibly different reflection sites for the upper and lower limbs. This may explain the difference in the age dependencies of the upper and lower limb RIs. On the other hand, the arteries of the lower limbs are longer but also more prone to develop atherosclerotic plaques than are the arteries in the upper limbs. The plaques causing either stiffening, stenosis or occlusions are more common with older people. Those changes in the major arteries of the lower limbs may attenuate the amplitude of the reflections so that practically only the stronger percussion wave caused

by the heartbeat passes through the arteries of the leg while the reflected wave is significantly attenuated [3]. In addition, the reflected waves arrive earlier due to increased pulse wave velocity caused by stiffened arteries as a result of aging. These two factors may cause highly overlapping percussion and reflected waves which result in difficulties at least in visual detection of the points of incisura and the reflected diastolic wave (Fig. 2). However, if these features are detected systematically as derivative based characteristic points in case of missing obvious local extremities, the amplitude of the feature considered as reflected diastolic wave increases in with respect to the percussion wave. For this reason, the individual parameters labeled in this study as reflection index (RI) may have different physiological background in case of the upper and lower limbs, although the required characteristic points can be detected in a similar way in both cases. This may be an explanation why there are differences in the age dependencies between the RIs determined from the arms and legs.

The p -values as a result of Mann-Whitney U-tests in Table IV and boxplots in Fig. 4 show that the individual parameter values from different age groups are strongly overlapped, whereas the combined parameters have better discrimination capability between different age groups. Also the variance inside each age group is clearly smaller with most of the combined parameters than with the individual parameters.

A notable issue is that the group of 40–69-year-old test subjects differs from younger with higher significance level than from the elders' group when analyzing the combined parameters. This can be explained by two factors: These middle-aged test subjects may have latent cardiovascular diseases with no symptoms whereas young people usually do not have such problems due to the strong age dependence of the prevalence of atherosclerosis. On the other hand, the age distributions of the young (group A) and middle-aged (group B) test subjects

are more distinct than the age distributions of middle-aged and elderly (group C) test subjects (Table I).

B. HR dependence

As seen in Table III, the average correlation coefficients between the parameter values and RR intervals are low, below 0.30 with all the parameters. If the age groups are studied separately, the strongest HR dependence is in the youngest age group A. This explains the large standard deviation of the HR correlation. The differences between the groups may be a result of respiratory sinus arrhythmia which is generally stronger in young healthy subjects. However, these small intra-subject variations can be eliminated by averaging the PW parameters over time, but the changes in the average HR between different measurements are more problematic. For these reasons, it is important that the subject being measured is in standard conditions, e.g. in rest and relaxed. In this study, the average instantaneous HR values of each study group are within 2 bpm (Table I) indicating that the HR does not significantly distort the analysis. Based on the obtained results, especially purely t_{pp} and RI based parameters indicate larger inter-subject variations due to HR than e.g. AGI and pAIx based parameters (Table III), although any clear HR dependence cannot be observed by a visual inspection of the results.

VI. CONCLUSIONS

We showed that our novel measurement system and analysis methods are capable of detecting the age-dependence of several pulse wave (PW) parameters from subjects with normal ABIs and without symptoms or previously diagnosed cardiovascular diseases. Altogether 14 out of 25 presented combined PW parameters have equal or stronger age-dependence with higher significance level than any of the tested individual 20 PW parameters for describing the arterial condition in the study population of 52 healthy 22–90-year-old test subjects with normal ABIs and without diagnosed cardiovascular diseases or symptoms. Also 13 combined parameters showed statistically significant differences between the 3 different age groups.

These findings can be utilized in future studies aiming for the development of non-invasive, fast and cheap diagnostic equipment for the detection of the patients at risk before they observe any symptoms. However, the strong age dependence in healthy subject population does not confirm that the parameters can be used in discriminating whether the patients do have atherosclerosis or not. In addition, the scaling of the parameters with respect to the HR may be a necessary step in our further studies although the inter-subject variation of the PW parameter values cannot be fully explained by the HR. Further investigation on this matter is required, and it will be an important part on our future work. Nevertheless, the study shows that combining the PW parameters from multiple measurement points and sensor modalities have unexploited potential in the PW analysis. In addition, the results encourage to implement analysis methods originally intended for PPG volume PWs also for pressure PWs and vice versa.

Further studies with e.g. atherosclerotic patients are needed and planned for finding out which analysis methods provide the most accurate results in discriminating whether the test subject has healthy or degenerated arteries.

VII. ACKNOWLEDGMENT

The authors would like to thank the volunteer test subjects for their valuable contribution to the study. The personnel in the polyclinics of the vascular diseases and especially research nurse Ritva Heikkinen from Oulu University Hospital are acknowledged for their contribution in recruiting test subjects and collecting the reference values.

REFERENCES

- [1] A. Alwan *et al.*, *Global status report on noncommunicable diseases 2010*. World Health Organization, 2011.
- [2] N. Oksala, J. Viljamaa, E. Saimanen, and M. Venermo, "Modified ankle-brachial index detects more patients at risk in a finnish primary health care," *European Journal of Vascular and Endovascular Surgery*, vol. 39, no. 2, pp. 227 – 233, 2010.
- [3] S. J. Ziemann, V. Melenovsky, and D. A. Kass, "Mechanisms, pathophysiology, and therapy of arterial stiffness," *Arteriosclerosis, Thrombosis, and Vascular Biology*, vol. 25, no. 5, pp. 932–943, 2005.
- [4] M. C. Baruch, K. Kalantari, D. W. Gerdt, and C. M. Adkins, "Validation of the pulse decomposition analysis algorithm using central arterial blood pressure," *Biomedical engineering online*, vol. 13, no. 1, p. 96, 2014.
- [5] U. Rubins, "Finger and ear photoplethysmogram waveform analysis by fitting with gaussians," *Medical & biological engineering & computing*, vol. 46, no. 12, pp. 1271–1276, 2008.
- [6] K. Takazawa, N. Tanaka, M. Fujita, O. Matsuoka, T. Saiki, M. Aikawa, S. Tamura, and C. Ibukiyama, "Assessment of vasoactive agents and vascular aging by the second derivative of photoplethysmogram waveform," *Hypertension*, vol. 32, no. 2, pp. 365–370, 1998.
- [7] K. Kohara, Y. Tabara, A. Oshiumi, Y. Miyawaki, T. Kobayashi, and T. Miki, "Radial augmentation index: a useful and easily obtainable parameter for vascular aging," *American journal of hypertension*, vol. 18, no. S1, pp. 11S–14S, 2005.
- [8] V. Melenovsky, B. A. Borlaug, B. Fetcs, K. Kessler, L. Shively, and D. A. Kass, "Estimation of central pressure augmentation using automated radial artery tonometry," *Journal of hypertension*, vol. 25, no. 7, pp. 1403–1409, 2007.
- [9] S. C. Millasseau, J. M. Ritter, K. Takazawa, and P. J. Chowienczyk, "Contour analysis of the photoplethysmographic pulse measured at the finger," *Journal of hypertension*, vol. 24, no. 8, pp. 1449–1456, 2006.
- [10] C. Liu, T. Zhuang, L. Zhao, F. Chang, C. Liu, S. Wei, Q. Li, and D. Zheng, "Modelling arterial pressure waveforms using gaussian functions and two-stage particle swarm optimizer," *BioMed Research International*, vol. 2014, 2014.
- [11] L. Wang, L. Xu, S. Feng, M. Q.-H. Meng, and K. Wang, "Multi-gaussian fitting for pulse waveform using weighted least squares and multi-criteria decision making method," *Computers in biology and medicine*, vol. 43, no. 11, pp. 1661–1672, 2013.
- [12] D. Goswami, K. Chaudhuri, and J. Mukherjee, "A new two-pulse synthesis model for digital volume pulse signal analysis," *Cardiovascular Engineering*, vol. 10, no. 3, pp. 109–117, 2010.
- [13] M. Peltokangas, A. Vehkaoja, J. Verho, M. Huotari, J. Rönning, and J. Lekkala, "Monitoring arterial pulse waves with synchronous body sensor network," *Biomedical and Health Informatics, IEEE Journal of*, vol. 18, no. 6, pp. 1781–1787, Nov 2014.
- [14] S. C. Millasseau, R. P. Kelly, J. M. Ritter, and P. J. Chowienczyk, "The vascular impact of aging and vasoactive drugs: comparison of two digital volume pulse measurements," *American journal of hypertension*, vol. 16, no. 6, pp. 467–472, 2003.
- [15] K. Takazawa, N. Tanaka, K. Takeda, F. Kurosu, and C. Ibukiyama, "Underestimation of vasodilator effects of nitroglycerin by upper limb blood pressure," *Hypertension*, vol. 26, no. 3, pp. 520–523, 1995.
- [16] K. Hoo, K. Tvarlapati, M. Piovoso, and R. Hajare, "A method of robust multivariate outlier replacement," *Computers & chemical engineering*, vol. 26, no. 1, pp. 17–39, 2002.